GeoStudio Example File
Frozen Ground Containment Barrier

To see the latest GeoStudio learning content, visit Seequent Learning Centre and search the catalogue for “GeoStudio”.

Introduction

Frozen soil barriers can be used to isolate contaminated water within a groundwater flow system. These barriers form as pore-ice decreases the hydraulic conductivity and causes water to divert around the frozen zone. Although heat conduction and dispersion occur through the frozen and unfrozen zones, heat advection (forced convection) with the flowing water supplements, and dominates, the heat transport in the unfrozen zone. A frozen wall example is used to illustrate the influence of groundwater flow on the propagation of a frozen soil barrier.

Numerical Simulation

McKenzie et al. (2007) developed a hypothetical scenario that is meant to represent a frozen wall boundary typically used in groundwater contamination remediation. The simulation is of warm groundwater flow across a 50 m long by 10 m high aquifer partially intersected by a 0.5 m wide by 5 m high frozen wall at an x-coordinate of 20 m. Figure 1 shows the domain and the applied boundary conditions. A temperature of -5°C is applied to the wall for the duration of the analysis. The left edge of the domain represents the upstream boundary where warm groundwater enters at a constant temperature of 5°C. Constant head boundary conditions of 10.05 m and 10.00 m are applied to the left and right-hand edges of the domain, respectively. Adiabatic conditions are assumed for the top, bottom, and right boundaries of the domain. The initial pore-water pressure distribution is developed using a steady-state water transfer analysis, while the initial temperatures are established using the activation temperature option that appears in the material model definition. An 800-day transient heat and water transfer simulation was completed on the same domain using an exponential time sequence with an initial one-day time increment. By default, the heat transfer analysis simulates conduction energy transfer. Toggling on the physics option for forced convection with water transfer introduces additional energy transfer mechanisms: heat advection as well as thermal dispersion with flowing water. As will later be shown, the frozen zone propagates both upstream and downstream, leading to an essentially impermeable zone that forces water to flow at a higher flux due to the decreasing surface area.

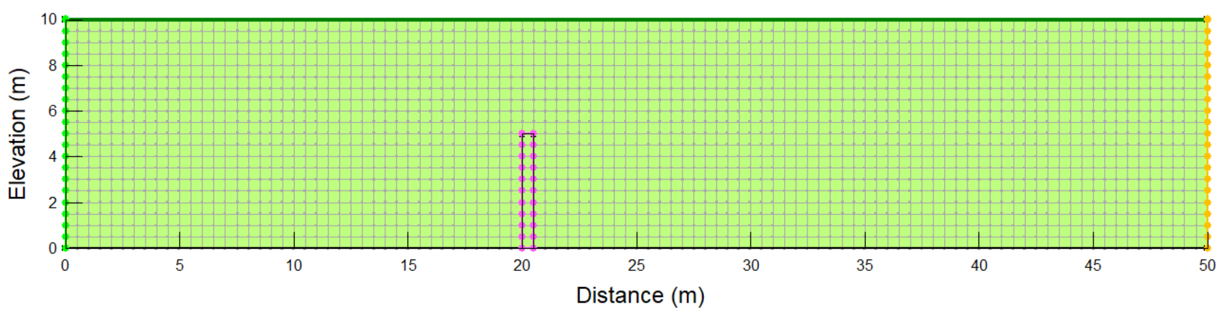

Figure 1. Problem configuration.

Clausnitzer and Mirnyy (2016) solved this problem using readily tractable properties and a non-zero gravity term. To follow suit, the full thermal material model is used and the normalized unfrozen volumetric water content function is defined using a simple ramp-type function:

$$\theta'_{uwc} = \begin{cases} 1 & T \geq T_o \\ (1 - \theta'_{uwc,r})\dfrac{T - (T_o - \Delta T)}{\Delta T} + \theta'_{uwc,r} & T_o \geq T > T_o - \Delta T \\ \theta'_{uwc,r} & T < T_o - \Delta T \end{cases} \quad \text{Equation 1}$$

where $\theta'_{uwc,r}$ is the residual normalized unfrozen volumetric water content, T is the temperature,

T_o is the phase change temperature, and ΔT is the phase change interval. The soil thermal conductivity is estimated using a weighted arithmetic mean:

$$k_t = \sum_{j=1}^{N} \theta_j k_{t,j} = \theta_w k_{t,w} + \theta_i k_{t,i} + \theta_s k_{t,s}$$ Equation 2

where $k_{t,j}$ is the thermal conductivity of the *j*th constituent, θ_j is the volumetric content (or volume fraction) of the *j*th constituent, $k_{t,w}$ is the thermal conductivity of water, θ_w is the volumetric water content, $k_{t,i}$ is the thermal conductivity of ice, θ_i is the volumetric ice content, $k_{t,s}$ is the thermal conductivity of the solid particles, $\theta_s = 1 - n$ is the volumetric solid particle content, and n is the porosity. The volumetric heat capacity is also estimated using a weighted arithmetic mean:

$$C = \sum_{j=1}^{N} \theta_j C_j = \theta_w C_w + \theta_i C_i + \theta_s C_s$$ Equation 3

where C_j is the volumetric heat capacity of the *j*th constituent, C_w is the volumetric heat capacity of water, C_i is the volumetric heat capacity of ice, and C_s is the volumetric heat capacity of the solid particles. Under frozen conditions, the volumetric water content is equal to the product of the normalized unfrozen volumetric water content and porosity while the volumetric ice content is equal to the remaining pore fraction, and more specifically, the difference between porosity and volumetric water content. Under unfrozen conditions, on the other hand, the volumetric water content is equal to porosity and the volumetric ice content is equal to zero. The analysis also accounts for hydrodynamic thermal dispersion. Table 1 provides the basic thermal properties used in these relationships.

Table 1. Basic thermal properties (Clausnitzer and Mirnyy, 2016).

Thermal Property	Value
Porosity	0.1
Thermal Conductivity of Water	0.0006 kJ/s/m/°C
Thermal Conductivity of Ice	0.00214 kJ/s/m/°C
Thermal Conductivity of Solid Particles	0.0035 kJ/s/m/°C
Volumetric Heat Capacity of Water	4182 kJ/m³/°C
Volumetric Heat Capacity Ice	2184 kJ/m³/°C
Volumetric Heat Capacity of Solid Particles	1939.36 kJ/m³/°C
Phase Change Temperature	1°C
Phase Change Interval	2°C
Residual Normalized Unfrozen Water Content	0.025
Longitudinal Dispersivity	5 m

Transverse Dispersivity	0.5 m

The water transfer formulation acknowledges the presence of pore ice in regions in which freezing occurs when (1) the forced convection physics option is toggled on, and (2) a saturated-unsaturated material model is used with the reduce conductivity in frozen ground checkbox toggled on. Figure 2 and Figure 3 show the volumetric water content and hydraulic conductivity functions of the aquifer. The volumetric water content function is estimated using Clapeyron's equation, porosity and the normalized unfrozen volumetric water content function. The hydraulic conductivity function is estimated using Clapeyron's equation and a ramp-type function of temperature in which the saturated and residual hydraulic conductivity is set equal to 1.11 x 10^{-3} and 1.11 x 10^{-9} m/sec, respectively. The hydraulic conductivity of the frozen or partially frozen soil is determined from the hydraulic conductivity function using the lesser (more negative) of the simulated or calculated (using Clapeyron's equation) pore-water pressure. In this example, the soil is completely saturated, and the negative pressure calculated with Clapeyron's equation is always used to determine the hydraulic conductivity of the frozen or partially frozen soil.

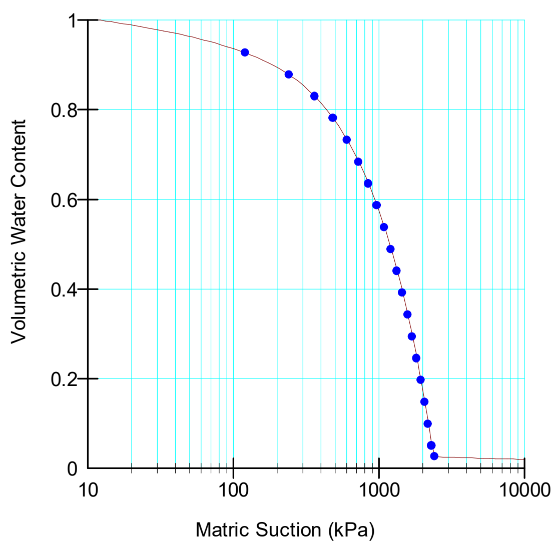

Figure 2. Volumetric water content function.

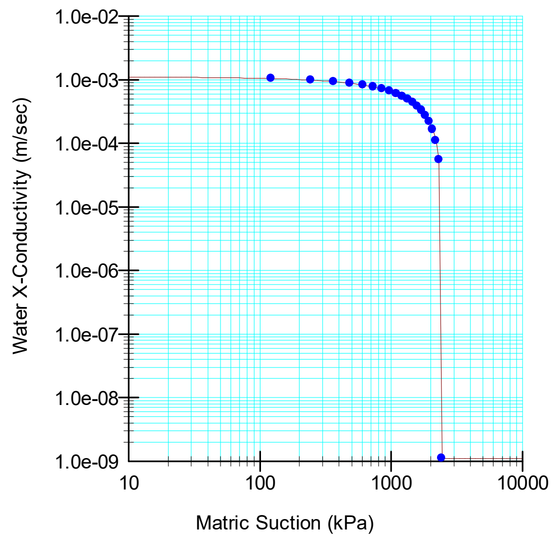

Figure 3. Hydraulic conductivity function.

Results and Discussion

Figure 4 shows the simulated temperature along the bottom of the domain after 4.2, 24.2, 56.2, 100, 200, 400 and 800 days. The freezing temperatures progress both upstream and downstream, until the upstream progression reaches a maximum that depends on the amount of water (and heat) flowing across the domain. The downstream temperatures continue to decrease as the vertical extent of the wall increases and the flow rate decreases.

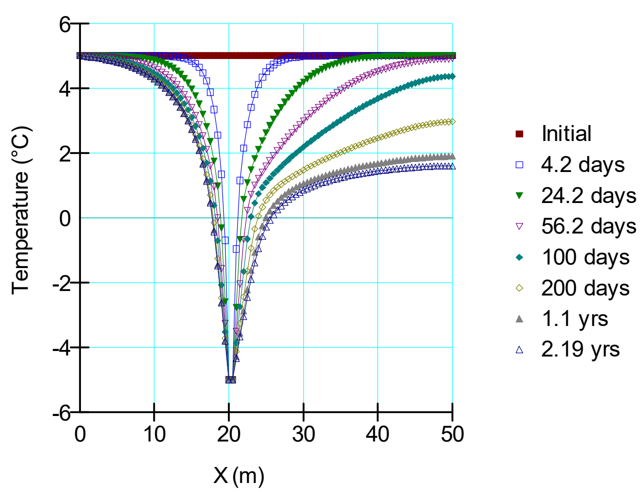

Figure 4. Temperature changes along the bottom of the domain.

As the frozen zone propagates outwards from the original wall, water is forced to flow through the unfrozen soil where the conductivity has not been reduced by pore-ice blockage. Fixing the total head on either side of the domain results in a constant gradient that leads to an overall decrease in water rate (and water volume) crossing the domain with decreasing surface area. To graph this decrease in water rate, a subdomain is graphed above the original wall. Figure 5 shows the subdomain drawn from the top of the wall to the upper limit of the domain. This allows for the creation of a graph of the rate of water moving into the elements of the subdomain. As shown in

Figure 6, the water rate decreases with time as pore ice blockage decreases the surface area. The water flux above the wall, on the other hand, increases relative to other parts of the domain due to the decrease in surface area, as is evidenced by the flow vectors.

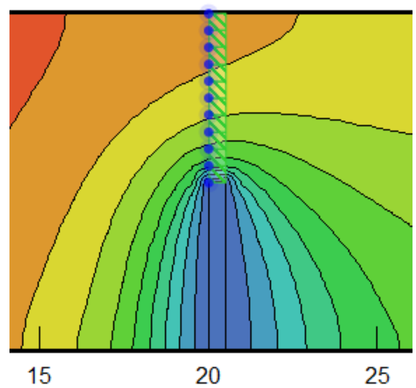

Figure 5. Subdomain cross section (in green) and node locations (in blue).

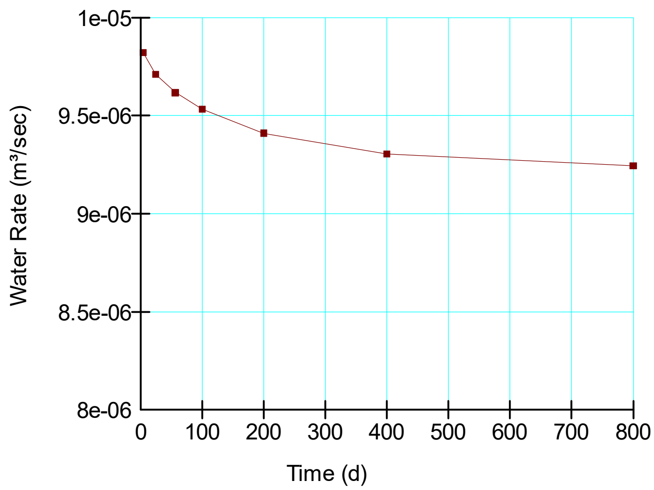

Figure 6. Cumulative water rate above the frozen wall.

Figure 7 shows the normalized unfrozen volumetric water content contour lines (in black), which are indicative of pore blockage. The zero-contour line delineates the region in which pores are filled with ice. In this case, the simple ramp-type function, in which water freezes over a small temperature range, leads to tightly spaced contour lines around the freeze wall. As expected, the contour lines are in very close agreement with the colored contours found in Clausnitzer and Mirnyy (2016).

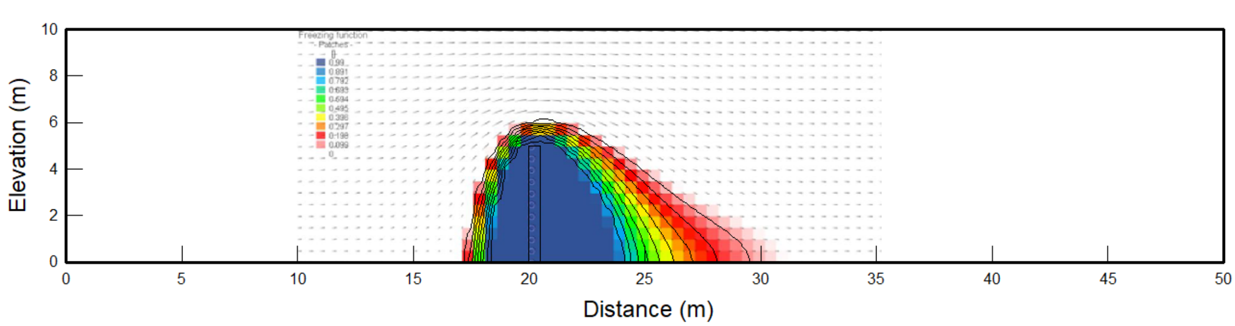

Figure 7. Normalized unfrozen volumetric water content contours on day 800.

Figure 8 shows the temperature contour lines after 4.2, 24.2, 56.2, 100, 200, 400 and 800 days. As with the normalized unfrozen volumetric water content contour lines, the contour lines (in black) are in very close agreement with the colored contours found in Clausnitzer and Mirnyy (2016). The upstream and downstream extent of the zero isotherm at the bottom of the domain eventually reaches 2 and 5 m from the wall, respectively. The larger extent of the freezing zone on the downstream side of the wall is mostly due to the heat transferred by advection (or forced convection). Although not shown here, a comparison of the results with/without thermal dispersion reveals that dispersion enhances heat transfer by accounting for fluid mixing and spreading in the presence of solid particles. Although the mixing and spreading is most significant in areas of high fluxes, such as above the wall, it occurs throughout the domain and allows for further propagation of the isotherms. The differences in results on the downstream side of the wall, which are most prevalent at early times, and likely due to differences in volumetric heat capacity. These results confirm the ability of the software to model transient conduction, convection, dispersion and phase change problems.

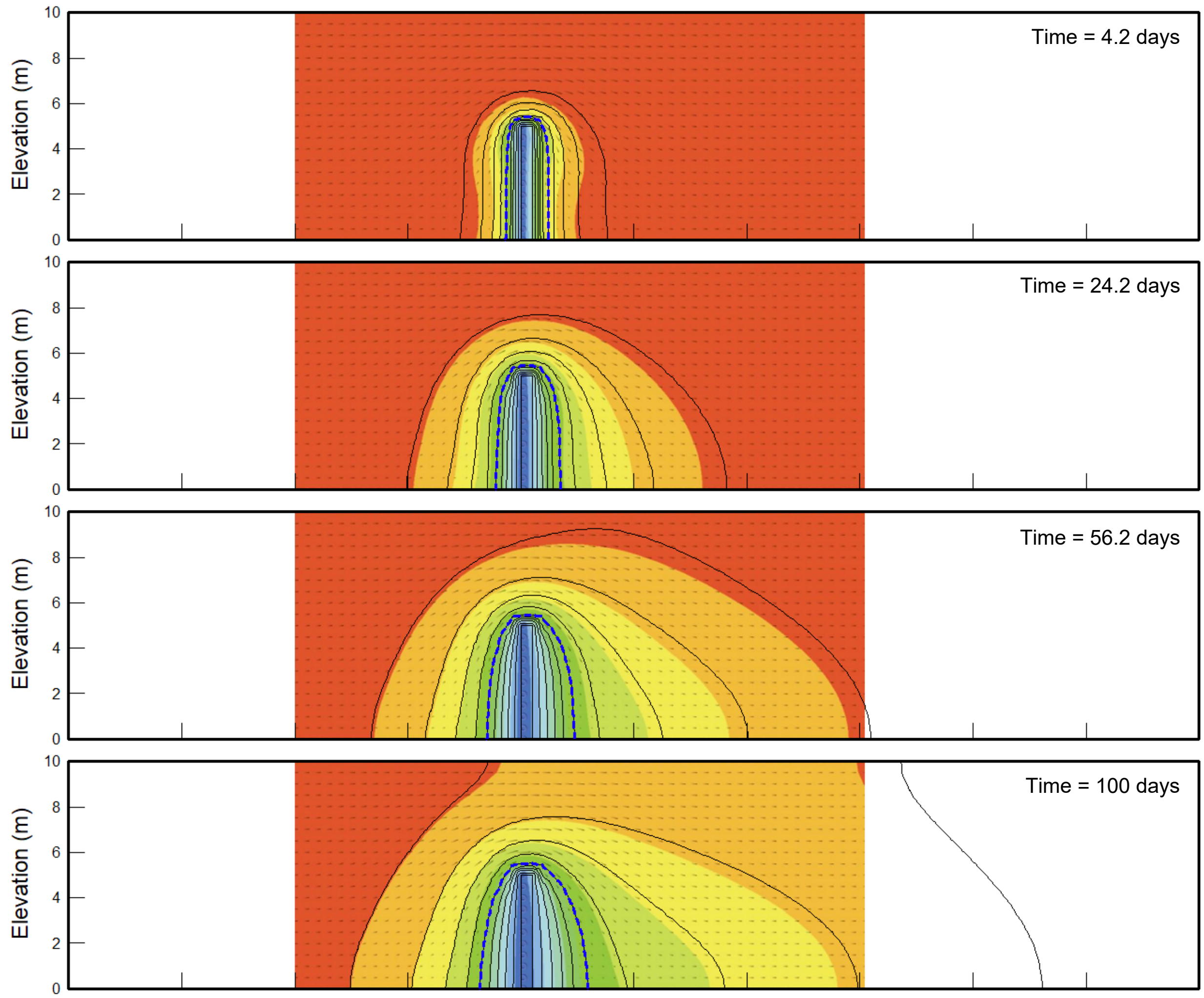

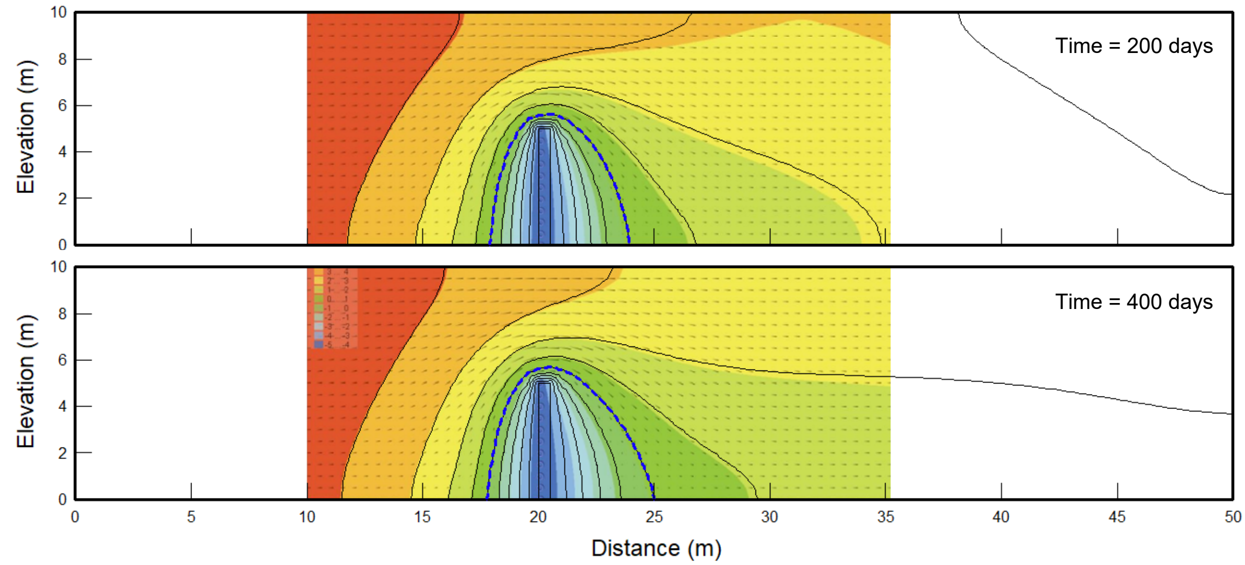

Figure 8. Temperature contours.

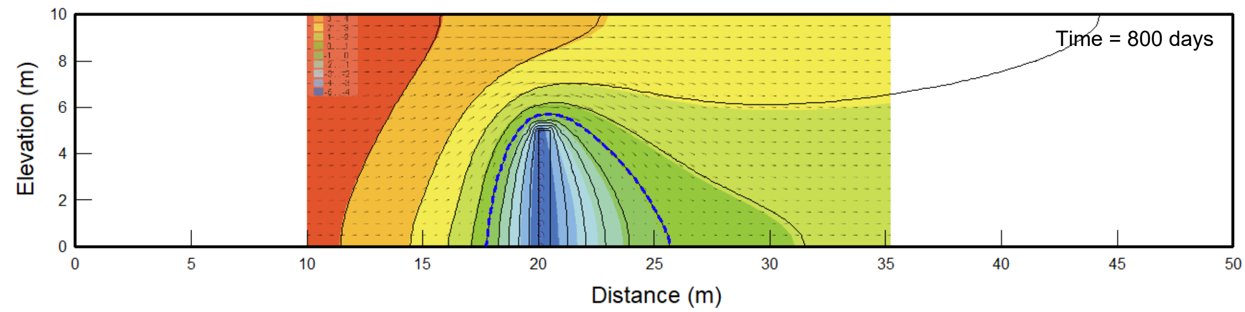

Figure 8. Temperature contours (continued).

Summary and Conclusions

A hydrothermal analysis was used to explore the effect of a penetrating frozen wall on the thermal and hydraulic regimes of a small aquifer. The analysis was based on an example proposed by McKenzie et al. (2007). The analysis revealed the significant role of ground freezing on groundwater flux, flow rate and patterns. As ice formation increased and hydraulic conductivity near the frozen wall decreased, water fluxes increased in the region above the wall. Upstream temperatures neared steady-state conditions more quickly given the constraints imposed by flowing groundwater, while downstream temperatures were more significantly influenced by advective heat transfer. Although thermal dispersion was most significant in areas of high fluxes, such as above the wall, it occurred throughout the domain and allowed for further propagation of the isotherms.

References

Clausnitzer, V., and Mirnyy, V. 2016. Modeling groundwater and heat flow subject to freezing and thawing. In: Proceedings of the International Mine Water Association Meeting, Leipzig, 11-15 July 2016. Edited by C. Drebenstedt, and M. Paul. Technische Universität Bergakademie, pp. 1150-1153.

McKenzie, J.M., Voss, C.I. and Siegel, D.I. 2007. Groundwater flow with energy transport and water-ice phase change: Numerical simulations, benchmarks, and application to freezing in peat bogs. Advances in Water Resources, 30(4): 966-983.